*Laser and Particle Beams* (2011), *29*, 365–372.

doi:10.1017/S0263034611000401

# Centroid and envelope dynamics of charged particle beams in an oscillating wobbler and external focusing lattice for heavy ion fusion applications

HONG QIN,[1,2] RONALD C. DAVIDSON,[1] AND B. GRANT LOGAN[3]

[1]Plasma Physics Laboratory, Princeton University, Princeton, New Jersey
[2]Department of Modern Physics, University of Science and Technology of China, Hefei, Anhui, China
[3]Lawrence Berkeley National Laboratory, Berkeley, California

(Received 12 September 2010; Accepted 20 June 2011)

**Abstract**

Recent heavy ion fusion target studies show that it is possible to achieve ignition with direct drive and energy gain larger than 100 at 1 MJ. To realize these advanced, high-gain schemes based on direct drive, it is necessary to develop a reliable beam smoothing technique to mitigate instabilities and facilitate uniform deposition on the target. The dynamics of the beam centroid can be explored as a possible beam smoothing technique to achieve a uniform illumination over a suitably chosen region of the target. The basic idea of this technique is to induce an oscillatory motion of the centroid for each transverse slice of the beam in such a way that the centroids of different slices strike different locations on the target. The centroid dynamics is controlled by a set of biased electrical plates called "wobblers." Using a model based on moments of the Vlasov-Maxwell equations, we show that the wobbler deflection force acts only on the centroid motion, and that the envelope dynamics are independent of the wobbler fields. If the conducting wall is far away from the beam, then the envelope dynamics and centroid dynamics are completely decoupled. This is a preferred situation for the beam wobbling technique, because the wobbler system can be designed to generate the desired centroid motion on the target without considering its effects on the envelope and emittance. A conceptual design of the wobbler system for a heavy ion fusion driver is briefly summarized.

**Keywords:** Centroid; heavy ion fusion; ignition; Oscillatory motion; Smoothing technique; Wobblers

## 1. INTRODUCTION

Recent heavy ion fusion target studies show that with appropriate beam energy ramp and beam smoothing techniques, it may be possible to achieve ignition with direct drive and energy gain larger than 100 at 1 MJ (Logan *et al.*, 2008). With the newly envisioned shock ignition method, it may be possible that an energy gain of 1000 could be achieved using 1.5 MJ heavy ion direct drive (Logan, 2011). To realize these advanced, high-gain heavy ion fusion schemes based on direct drive, it is important to develop a reliable beam smoothing technique to mitigate instabilities and facilitate uniform deposition. It has been proposed recently that the dynamics of the beam centroid can be explored as a possible beam smoothing technique (Hoffmann, 2009; Logan *et al.*, 2008; Qin & Davidson, 2009; Qin *et al.*, 2010; Sharkov, 2007; Tahir *et al.*, 2001, 2010) to achieve a uniform illumination over a suitably chosen region of the target. The basic idea of this technique is to induce an oscillatory motion of the centroid for each transverse slice of the beam in such a way that the centroids of different slices strike different locations on the target. The centroid of different slices projected onto the target follows a smooth pattern to achieve the desired uniform illumination over a suitably chosen region, e.g., an annular region, for significantly, improved stability properties during the target implosion phase (Kawata *et al.*, 1993; Logan *et al.*, 2008; Piriz *et al.*, 2003*a*, 2003*b*). The improvement of stability properties can be attributed to two factors. First, uniform illumination reduces the initial seeding amplitude of the Rayleigh-Taylor instability. Second, at a given location on the target, the energy/momentum input is pulsating rapidly with time, which results in a dynamic stabilization effect for the instability.

Address correspondence and reprint requests to: Hong Qin, Plasma Physics Laboratory, Princeton University, Princeton, NJ 08543. E-mail: hongqin@princeton.edu

The centroid dynamics is actively controlled by the deflection force imposed by a set of biased electrical plates. They are called "wobblers," because of the wobbling motion that these places induce for the beam centroid. The bias voltage on the wobbler plates needs to oscillate with time in order to deliver different beam slices to different locations (See Fig. 1). The wobbling motion is generated before the final focusing at the upstream, and the $x$–deflector the $y$–deflectors can be interlaced. In the research of laser-driven inertial confinement fusion, smoothing systems using distributed phase-plate technology have been developed to achieve uniform laser illumination (Skupsky *et al.*, 1993). The wobbler system for charged beams in the present study is analogous to these smoothing systems for laser beams.

Beam dynamics is usually studied in terms of envelope and centroid motions (Barnard, 1996; Lee *et al.*, 1988; Lund & Barnard, 2009; Lund & Bukh, 2004; Sharp *et al.*, 1992). However, motions of the centroid and envelope represent different degrees of freedom. The most common applications of the envelope dynamics is to design beam focusing systems (Friedman *et al.*, 2009; Qin *et al.*, 2004), while the study of centroid dynamics is mainly to minimize the oscillations of the beam centroid around the design orbit (Blind & Gilpatrick, 2007). In terms instabilities, two-stream electron cloud instability (Neuffer *et al.*, 1992; Zimmermann, 2004) can be modeled by the centroid dynamics, and unstable breathing modes can be described by envelope instabilities (Bernal *et al.*, 2006; Lund & Bukh, 2004). It is easy to show that the centroid dynamics and the envelope dynamics are decoupled, if the space-charge force is weak. In this case, the centroid dynamics is governed by the dynamical equations for a singled charged particle moving in the external focusing lattice and wobbler fields. However, for heavy ion fusion, the beam intensity is often high, and the self-generated space-charge force should be considered when determining the governing equations for the centroid dynamics. It is especially crucial to determine whether the centroid dynamics and the envelope dynamics are coupled. Another issue needs to be addressed is whether a realistic wobbler system using technologies that are currently available can be designed to achieve the required wobbler motion. We will study these important questions regarding the centroid and envelope dynamics of charged particle beams in a wobbler field and an external focusing lattice.

We start our study from the nonlinear Vlasov-Maxwell equations for high-intensity beams (Davidson & Qin, 2001) in a wobbler field and an external focusing lattice, using two different approaches. In the first approach, a set of rate equations for the centroid and the root-mean-square (rms) envelope and emittance is derived by taking moments of the Vlasov-Maxwell equations. The second approach is to construct a generalized self-consistent solution of the Vlasov-Maxwell equations that includes both envelope dynamics and centroid dynamics. This kinetic solution is similar to the Kapchinskij-Vladimirskij (KV) (Kapchinskij & Vladimirskij, 1959) in construction. The external deflection force induced by the wobbler fields is included in the models, in addition to the transverse focusing lattice. Since the Vlasov-Maxwell equations are nonlinear, adding this additional physics could result in unexpected results. In order to systematically study the wobbler dynamics, we need to carry out a careful analysis of the Vlasov-Maxwell equations including simultaneously all of the relevant physics components, i.e., the wobbler fields, the focusing lattice, the space-charge force,

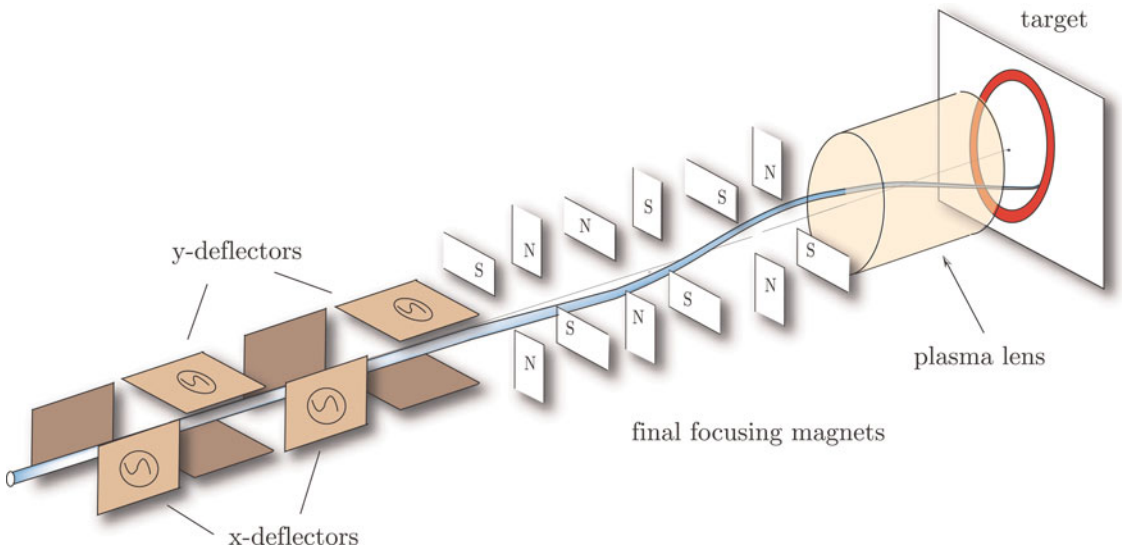


**Fig. 1.** (Color online) Wobbler system and quadrupole focusing lattice with neutralizing plasma lens. The bias voltage on the wobbler plates oscillates with time to deliver different beam slices to different locations on the target. The projected motion of the centroid on the target follows a smooth pattern to achieve uniform illumination over a suitably chosen region of the target. The $x$–deflector the $y$–deflectors can be interlaced.

https://doi.org/10.1017/S0263034611000401 Published online by Cambridge University Press

and the emittance. Using these two models, we show that the wobbler deflection force acts only on the centroid motion, and that the envelope dynamics is independent of the wobbler fields. Furthermore, if the conducting wall is far away from the beam, then the envelope dynamics and the centroid dynamics are completely decoupled even when the space-charge force is strong. Based on these models, a conceptual design of the wobbler system for a heavy ion fusion driver is outlined. We demonstrate that a 10-meter-long, 67 MHz reversed field (RF) with 0.30 MV/m field strength is able to impose enough transverse momentum to generate the desired wobbler motion on a 2.5 mm target plane for a 2.43 GeV $Cs^+$ beam with a 2895 A peak current.

This paper is organized as follows. In Section 2, the moment equations for the beam centroid and envelope are derived from the nonlinear Vlasov-Maxwell equations. The self-consistent kinetic solution and associated centroid and envelope equations are presented in Section 3. We outline a conceptual design example for the heavy ion fusion wobbler and final focusing system in Section 4.

## 2. MOMENT EQUATIONS FOR THE CENTROID AND ENVELOPE

The transverse dynamics of a particle in a quadrupole focusing lattice with wobbler fields is governed by (Davidson & Qin, 2001)

$$x'' = -\kappa_x(s)x - \frac{\partial \psi}{\partial x} + F_x(s), \tag{1}$$

$$y'' = -\kappa_y(s)y - \frac{\partial \psi}{\partial y} + F_y(s). \tag{2}$$

Here, $(x, y)$ are the transverse coordinates in the laboratory frame, $\psi = e\phi/\gamma^3 m\beta^2 c^2$ is the normalized self-field potential, $\kappa_x(s) = -\kappa_y(s) = \kappa_q(s)$ are the focusing strengths of the quadrupole lattice, and $F_x(s)$ and $F_y(s)$ are the transverse deflection forces of the wobblers. The nonlinear Vlasov-Maxwell equations for the beam distribution function $f(s, x, y, v_x, v_y)$ and self-field potential $\psi$ are (Davidson & Qin, 2001)

$$\frac{\partial f}{\partial s} + v_x\frac{\partial f}{\partial x} + v_y\frac{\partial f}{\partial y} - \left(\kappa_x x + \frac{\partial \psi}{\partial x} - F_x\right)\frac{\partial f}{\partial v_x} - \left(\kappa_y y + \frac{\partial \psi}{\partial y} - F_y\right)\frac{\partial f}{\partial v_y} = 0, \tag{3}$$

$$\left(\frac{\partial^2}{\partial x^2} + \frac{\partial^2}{\partial y^2}\right)\psi = -\frac{2\pi K_b}{N_b}\int f\, dv_x dv_y, \tag{4}$$

where $N_b = \int f dv_x dv_y dx dy$ is the line density of the beam particles, and $K_b = 2N_b e^2/\gamma^3 m\beta^2 c^2$ is the self-field perveance. Here, $m$ is the rest mass of a beam particle, $\gamma$ is the relativistic mass factor, $c$ is the speed of light in *vacuo*, and $\beta c$ is the beam velocity. It is assumed in this model that there is no longitudinal coupling between different slices of the beam, and Eqs. (3) and (4) describe the transverse dynamics of each slice of the beam.

Our first objective is to derive the rms envelope equations and the centroid equations (Barnard, 1996 ; Lee *et al.*, 1988; Lund & Barnard, 2009; Lund & Bukh, 2004; Sharp *et al.*, 1992) by taking phase-space moments of the Vlasov equation. For any phase-space function $\chi(x, y, v_x, v_y, s)$, the $\chi$-moment of $f$ is defined as

$$\langle\chi\rangle \equiv (\int \chi f\, dxdydv_xdv_y)/N_b. \tag{5}$$

From the Vlasov Eq. (3), we obtain (Davidson & Qin, 2001) the rate equation for $\langle\chi\rangle$

$$\frac{d\langle\chi\rangle}{ds} = \langle\frac{\partial\chi}{\partial s} + v_x\frac{\partial\chi}{\partial x} + v_y\frac{\partial\chi}{\partial y} - \left(\kappa_x x + \frac{\partial\psi}{\partial x} - F_x\right)\frac{\partial\chi}{\partial v_x} - \left(\kappa_y y + \frac{\partial\psi}{\partial y} - F_y\right)\frac{\partial\chi}{\partial v_y}\rangle. \tag{6}$$

The transverse displacement of the beam centroid is defined by the first moment of $f$ with respect to displacement, i.e.,

$$\mu \equiv \langle x\rangle, \tag{7}$$

$$\nu \equiv \langle y\rangle. \tag{8}$$

Applying Eq. (6), we obtain

$$\mu' = \langle x\rangle' = \langle x'\rangle = \langle v_x\rangle, \tag{9}$$

$$\nu' = \langle y\rangle' = \langle y'\rangle = \langle v_y\rangle. \tag{10}$$

Taking $\chi = v_x$ and $\chi = v_y$ in Eq. (6), we acquire the centroid dynamical equations

$$\mu'' = \langle v_x\rangle' = -\kappa_x\mu + F_x - \langle\frac{\partial\psi}{\partial x}\rangle, \tag{11}$$

$$\nu'' = \langle v_y\rangle' = -\kappa_y\nu + F_y - \langle\frac{\partial\psi}{\partial y}\rangle. \tag{12}$$

It turns out that the rms envelope dimensions $(a, b)$ and transverse emittances $(\varepsilon_x, \varepsilon_y)$ need to be defined relative to the centroid as

$$a \equiv \sqrt{\langle x-\mu\rangle^2},$$
$$\varepsilon_x \equiv 2\sqrt{a^2\langle(v_x-\mu')^2\rangle - \langle(v_x-\mu')(x-\mu)\rangle^2}, \tag{13}$$
$$b \equiv \sqrt{\langle y-\nu\rangle^2},$$
$$\varepsilon_y \equiv 2\sqrt{b^2\langle(v_y-\nu')^2\rangle - \langle(v_y-\nu')(y-\nu)\rangle^2}. \tag{14}$$

To derive the dynamics equations for $a$, we need the rate equations for $\chi = (x-\mu)^2/2$ and $\chi = (v_x-\mu')(x-\mu)$. For

https://doi.org/10.1017/S0263034611000401 Published online by Cambridge University Press

$\chi = (x-\mu)^2/2$, the rate equation is

$$\frac{1}{2}\frac{d}{ds}\langle (x-\mu)^2\rangle = \frac{d}{ds}\frac{a^2}{2} = \langle -(x-\mu)\frac{\partial \mu}{\partial s}\rangle + \langle x'(x-\mu)\rangle + \langle (x'-\mu')(x-\mu)\rangle. \quad (15)$$

For $\chi = (v_x - \mu')(x-\mu)$, the corresponding rate equation is

$$\frac{d}{ds}\langle (v_x-\mu')(x-\mu)\rangle = \langle (x'-\mu')^2\rangle - \kappa_x(s)\langle (x-\mu)^2\rangle - \langle \frac{\partial \psi}{\partial x}(x-\langle x\rangle)\rangle + \langle F_x(x-\mu)\rangle. \quad (16)$$

Taking another time-derivative on Eq. (15), we obtain

$$\begin{aligned}\frac{d^2}{ds^2}\frac{a^2}{2} &= \frac{d}{ds}\langle (x'-\mu')(x-\mu)\rangle \\ &= \langle (x'-\mu')^2\rangle - \kappa_x(s)\langle (x-\mu)^2\rangle \\ &\quad - \langle \frac{\partial \psi}{\partial x}(x-\mu)\rangle + \langle F_x(x-\mu)\rangle. \end{aligned} \quad (17)$$

According the definition of $\varepsilon_x$ in Eq. (13), the $\langle (x'-\mu')^2\rangle$ term on the right-hand side of Eq. (17) can be expressed as

$$\langle (x'-\mu')^2\rangle = \frac{\varepsilon_x^2}{4a^3} - \left(\frac{da}{ds}\right)^2. \quad (18)$$

Then Eq. (17) can be re-written as the envelope equation for $a$,

$$a'' + \kappa_x a + \frac{\varepsilon_x^2}{4a^3} - \frac{1}{a}\langle \frac{\partial \psi}{\partial x}(x-\mu)\rangle. \quad (19)$$

To derive the dynamical equation for $\varepsilon_x$, we need the rate equation for $\chi = (v_x-\mu')^2$, i.e.,

$$\frac{d}{ds}\langle (v_x-\mu')^2\rangle = \langle 2(x'-\mu')\left(-k_s(s)x - \frac{\partial \psi}{\partial x} + F_x\right)\rangle. \quad (20)$$

From the definition of $\varepsilon_x$, the time-derivative of $\varepsilon_x^2$ is

$$\begin{aligned}\frac{d}{ds}\frac{\varepsilon_x^2}{4} &= a^2\frac{d}{ds}\langle (x'-\mu')^2\rangle + \langle (x'-\mu')^2\rangle\frac{da^2}{ds} \\ &\quad - 2\langle (x'-\mu')(x-\mu)\rangle\frac{d}{ds}\langle (x'-\mu')(x-\mu)\rangle. \end{aligned} \quad (21)$$

Making use of Eq. (20), Eq. (21) can be simplified to

$$\frac{d}{ds}\left(\frac{\varepsilon_x^2}{8}\right) = \langle \frac{\partial \psi}{\partial x}(x-\mu)\rangle\frac{d}{ds}\left(\frac{a^2}{2}\right) - a^2\langle \frac{\partial \psi}{\partial x}(v_x-\mu')\rangle. \quad (22)$$

Eqs. (19) and (22) are the envelope equations for $a$ and $\varepsilon_x$. Similarly, the dynamical equations for $b$ and $\varepsilon_y$ can be derived, and expressed as

$$b'' + \kappa_x b = \frac{\varepsilon_y^2}{4b^3} - \frac{1}{b}\langle \frac{\partial \psi}{\partial y}(y-\nu)\rangle, \quad (23)$$

$$\frac{d}{ds}\left(\frac{\varepsilon_y^2}{8}\right) = \langle \frac{\partial \psi}{\partial y}(y-\nu)\rangle\frac{d}{ds}\left(\frac{b^2}{2}\right) - b^2\langle \frac{\partial \psi}{\partial y}(v_y-\nu')\rangle. \quad (24)$$

Eqs. (11), (12), (19), and (22)–(24) forms a equation system to determine the evolution of the centroid, the rms envelope dimensions, and the transverse emittances. Eqs. (19) and (23) indicate that the deflection force of the wobbler fields does not affect directly the dynamics of envelope and emittances. If the conducting wall is far away from the beam, then the image-charge effects are negligible. In this case, we can show that the self-field terms in Eqs. (11) and (12) vanish (see Eq. (28)), and the self-field potential $\psi$ is a function of $(x-\mu, y-\nu)$ only. It is clear then that the self-field force does not affect the centroid, and the dynamics of the envelope dimensions and emittances is independent of the centroid. The dynamics of the centroid, envelope dimensions, and emittances are completely decoupled. The centroid motion is controlled only by the focusing lattice and wobbler fields, and the envelope dimensions and emittances defined relative to the centroid evolve as if there were no wobbler fields. This is a preferred situation for the proposed beam wobbling technique. The wobbler system can be designed to generate the desired centroid motion on the target without considering it effects on the envelope and emittance.

On the other hand, if the conducting wall is close to the beam, the dynamics of the centroid, envelope dimensions and emittances will be coupled by the self-field force. To determine the effects of the self-field on the centroid, we note that in Eqs. (11) and (12) the self-field force is

$$\begin{aligned}-\left(\langle \frac{\partial \psi}{\partial x}\rangle, \langle \frac{\partial \psi}{\partial y}\rangle\right) &= -\langle \nabla\psi\rangle = \int -f\nabla\psi dv_x dv_y dx dy \\ &= -\int_V n\nabla\psi dx dy. \end{aligned} \quad (25)$$

Using the fact that

$$\begin{aligned}-n\nabla\psi &= \frac{N_b}{2\pi K_b}(\nabla\cdot\nabla\psi)\nabla\psi \\ &= \frac{N_b}{2\pi K_b}\left[\nabla\cdot(\nabla\psi\nabla\psi) - (\nabla\psi\cdot\nabla)\nabla\psi\right] \end{aligned} \quad (26)$$

and

$$\nabla\frac{|\nabla\psi|^2}{2} = (\nabla\psi\cdot\nabla)\nabla\psi, \quad (27)$$

we can express the self-field force as a surface integral over the conducting wall,

$$-\langle \nabla\psi\rangle = \frac{N_b}{2\pi K_b}\int_{wall}\left(\nabla\psi\nabla\psi - |\nabla\psi|^2\mathbf{I}\right)\cdot d\mathbf{s}. \quad (28)$$

https://doi.org/10.1017/S0263034611000401 Published online by Cambridge University Press

Here **I** is the unit tensor. Eq. (28) states that the self-field force on the centroid motion is determined by the self-field on the conducting wall. If the conducting wall approaches infinity, the self-field force vanishes, which agrees with our previous estimate. The equations employed in CIRCE code (Sharp *et al.*, 1992) show that the centroid and envelope equations become decoupled when the pipe radius is set to infinity. The self-field potential $\psi$ will depend on $(x-\mu, y-\nu)$ as well as $(\mu, \nu)$ if the conducting wall is nearby, which means that the centroid dynamics will affect the dynamics of the envelope dimensions and emittances. This effect can be viewed as the image charge effect, and should be minimized in the design of wobbler systems. The image charge effect has been previously analyzed (Lee *et al.*, 1988).

In the present study, we assume that the conducting wall is far away from the beam and define the envelope dimensions and emittances relative to the centroid (See Eqs. (13) and (14)). Then the envelope equations and the emittance equations are exactly the same as those in the laboratory coordinate system in the absence of centroid dynamics (Qin *et al.*, 2010). Therefore, known results for the case without centroid and wobbler fields can be applied directly to Eqs. (19) and (22)–(24). In terms of envelope equation, an important result is for beams with fixed-shape density profiles. If for all time the beam density profile has the following fixed-shape form

$$n(X, Y, s) = \frac{N_b}{2\pi ab} S\left(\frac{X^2}{2a^2} + \frac{Y^2}{2b^2}\right), \tag{29}$$

where $S$ is the density shape function, it can then be shown (Davidson & Qin, 2001) that the beam emittance is a constant of motion and the envelope Eqs. (19) and (23) reduce exactly to

$$a'' + \kappa_x a = \frac{\varepsilon_x^2}{4a^3} - \frac{K_b}{2(a+b)}, \tag{30}$$

$$b'' + \kappa_x a = \frac{\varepsilon_y^2}{4b^3} - \frac{K_b}{2(a+b)}. \tag{31}$$

The difference between Eqs. (30) and (31) and Eqs. (19) and (23) is that Eqs. (30) and (31) form a closed set of equations for the envelope dimensions $(a, b)$, and Eqs. (19) and (23) do not.

## 3. SELF-CONSISTENT KINETIC DISTRIBUTION AND ASSOCIATED CENTROID AND ENVELOPE EQUATIONS

In the last section, we showed that when the conducting wall is far away, the envelope equations relative to the centroid is similar to the those without the centroid freedom. Since for the later case there is a corresponding self-consistent KV solution of the nonlinear Vlasov-Maxwell equations, this similarity suggests that a self-consistent solution of the nonlinear Vlasov-Maxwell equations similar to the KV solution may exist for high-intensity beams including the centroid dynamics in a wobbler field and an external focusing lattice. In this section, we show that such a self-consistent kinetic solution indeed exists, and it is similar to the KV solution in phase-space structure (Qin *et al.*, 2010).

Because the self-field potential $\psi$ and the distribution function is nonlinearly coupled in the Vlasov-Maxwell equations, to construct the self-consistent solution, we first assume a specific form for the density profile to determine the self-field potential $\psi$, and find the invariants of the particle dynamics in the external field and the self-field. Any function of the invariants as a distribution function in the phase space is a solution of the Vlasov equation. However, an arbitrary distribution function constructed this way will not generate the density profile assumed. We will select a specific distribution function of the invariants and verify that it indeed generates the initially assumed self-field potential $\psi$. Then a self-consistent solution is found, and the Vlasov-Maxwell equations in the phase space are reduced to a set of envelope equations that are ordinary differential equations in terms of time. For a high-intensity beam in a wobbler field and a quadrupole lattice, we start by assuming that beam density is constant inside the ellipse centered at $(\mu, \nu)$ with dimension $(\bar{a}, \bar{b})$ and vanishes outside the ellipse, i.e.,

$$n = \begin{cases} N_b/\pi\bar{a}\bar{b}, & X^2/a^2 + Y^2/b^2 \le 1, \\ 0, & X^2/a^2 + Y^2/b^2 > 1, \end{cases} \tag{32}$$

where $X \equiv x - \mu$ and $Y \equiv y - \nu$ are the displacement relative to the centroid (See Fig. 2). The corresponding self-field is linear in the centroid frame,

$$\frac{\partial\psi}{\partial x} = \frac{-2K_b(x-\mu)}{\bar{a}(\bar{a}+\bar{b})}, \quad \frac{\partial\psi}{\partial y} = \frac{-2K_b(y-\nu)}{\bar{b}(\bar{a}+\bar{b})}, \tag{33}$$

which is equivalent to assume the self-field potential to be

$$\psi = -\frac{K_b}{(\bar{a}+\bar{b})}\left[\frac{(x-\mu)^2}{\bar{a}^2} + \frac{(y-\nu)^2}{\bar{b}^2}\right]. \tag{34}$$

The dynamics of $(\mu, \nu)$ and $(\bar{a},\bar{b})$ in above equations need to be determined. Obviously, $\bar{a}$ and $\bar{b}$ are related to the rms envelope dimensions $a$ and $b$ through $\bar{a} = \sqrt{2}a$ and $\bar{b} = \sqrt{2}b$. For the centroid dynamics, we let the centroid motion satisfy

$$\mu'' + \kappa_x\mu - F_x = 0, \tag{35}$$

$$\nu'' + \kappa_y\nu - F_y = 0. \tag{36}$$

https://doi.org/10.1017/S0263034611000401 Published online by Cambridge University Press

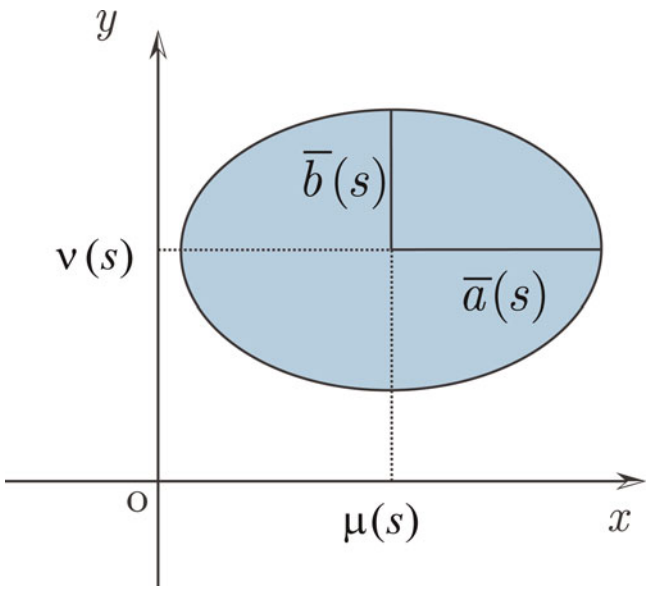


**Fig. 2.** (Color online) Beam density is constant inside the ellipse centered at $(\mu, \nu)$ with dimension $(\bar{a},\bar{b})$ and vanishes outside the ellipse.

From Eqs. (1), (2), (35), and (36) evolve according to

$$X'' + \left[\kappa_x - \frac{2K_b}{\bar{a}(\bar{a}+\bar{b})}\right]X = 0, \tag{37}$$

$$Y'' + \left[\kappa_y - \frac{2K_b}{\bar{b}(\bar{a}+\bar{b})}\right]Y = 0. \tag{38}$$

Since Eqs. (37) and (38) are linear in $X$ and $Y$, they admit the Courant-Snyder invariants for the $X$ and $Y$ motions, i.e.,

$$A_X = \frac{\varepsilon_x^2 X^2}{\bar{a}^2} + \varepsilon_x^2\left(\bar{a}X' - X\bar{a}'\right)^2 = const.,$$

$$A_Y = \frac{\varepsilon_y^2 Y^2}{\bar{b}^2} + \varepsilon_y^2\left(\bar{b}Y' - Y\bar{b}'\right)^2 = const., \tag{39}$$

where $\varepsilon_x$ and $\varepsilon_y$ are constants corresponding to the conserved transverse emittances, and $\bar{a}$ and $\bar{b}$ are determined from the envelope equations

$$\bar{a}'' + \kappa_x\bar{a} - \frac{2K_b}{(\bar{a}+\bar{b})} = \frac{\varepsilon_x^2}{\bar{a}^3}, \tag{40}$$

$$\bar{b}'' + \kappa_y\bar{b} - \frac{2K_b}{(\bar{a}+\bar{b})} = \frac{\varepsilon_y^2}{\bar{b}^3}. \tag{41}$$

Because $A_x$ and $A_y$ are constant of motion, any function of $A_x$ and $A_y$ is an exact solution of the Vlasov equation (3). But we also need the distribution function to generate flat-top density profile assumed in Eq. (32). We now show that the choice of distribution function (Davidson & Qin, 2001)

$$f = \frac{N_b}{\pi^2\varepsilon_x\varepsilon_y}\delta\left(\frac{A_X}{\varepsilon_x} + \frac{A_Y}{\varepsilon_y} - 1\right) \tag{42}$$

has this property. To verify this fact, we calculate the beam density from $f$,

$$n(X, Y, s) = \int f dv_x dv_y = \begin{cases} N_b/\pi\bar{a}\bar{b}, & X^2/a^2 + Y^2/b^2 \le 1, \\ 0, & X^2/a^2 + Y^2/b^2 > 1. \end{cases} \tag{43}$$

This is exactly the same as in Eq. (32). The distribution function given by Eq. (42) has the same structure as the KV distribution in the phase-space. We note that this kinetic distribution does not follow directly from the moment equations for the envelope and centroid in Section 2, because the moment equations do not specify the distribution function. Finding a distribution function that solves the Vlasov-Maxwell equations is generally non-trivial, and a closed set of envelope and emittance equations does not guarantee the existence of an exact kinetic solution in the phase-space. Working together, with the moment equations and the KV solution give a leading-order description of the wobbler dynamics.

## 4. CONCEPTUAL DESIGN EXAMPLE OF A HEAVY ION FUSION WOBBLER AND FINAL FOCUSING SYSTEM

As an example, we give a conceptual design of a final focus and wobbler system for a heavy ion fusion driver. The layout of the system is illustrated in Figure 3. The beam is a $Cs^+$ beam with rest mass $m = 132.9$ au, kinetic energy $(\gamma - 1)$ $mc^2 = 2.43$ GeV, and current $I = 2895$ A. These parameters are for a typical heavy ion fusion driver design described in Qin *et al.* (2004). At $s = 0$ the wobbler fields (not shown) imposes a transverse momentum to the beam centroid. The beam is then focused onto the target at $s = 19$ m, with transverse spot size $a = b = 1.2$ mm after propagating through the final focus magnets with focusing strength $\kappa_q$ $(s)$, whose strength is denoted by $\kappa_q$ $(s)$ in Figure 3. The normalized strength $\hat{\kappa}_q$ of the four quadrupole magnets is $0.13\ \mathrm{m}^{-2}$, $0.22\ \mathrm{m}^{-2}$, $0.44\ \mathrm{m}^{-2}$, and $-0.47\ \mathrm{m}^{-2}$. The initial envelope dimensions at $s = 0$ are $(a, b) = (4$ cm, $2.28$ cm). The region between $s = 11$ m and $s = 19$ m is filled with preformed plasma which neutralizes the space-charge potential of the beam, but not the current (Friedman *et al.*, 2009). In this region, the size of the beam continues to decrease before it strikes on the target. This is of course the effect of a plasma lens. The wobbler fields induce different transverse momenta for different slices according to oscillatory sinusoidal forces at $s = 0$. The forces in the $x$- and $y$-directions has a $\pi/2$ phase difference. Therefore, the beam centroid traces out a circle on the target. The centroid dynamics illustrated in Figure 3 corresponds to the slice where $(\mu, \nu) = (1.77$ mm, $1.77$ mm) on the target, and the normalized momentum input by the wobbler fields is $(\mu', \nu') = (6.27 \times 10^{-4}, -0.85 \times 10^{-4})$ at $s = 0$. The radius of the centroid circle is 2.5 mm. The required frequency of the wobbler fields is 67 MHz for a beam pulse of 15 ns long. If the effective length of the wobbler field is 10 m, the RF field strength

https://doi.org/10.1017/S0263034611000401 Published online by Cambridge University Press

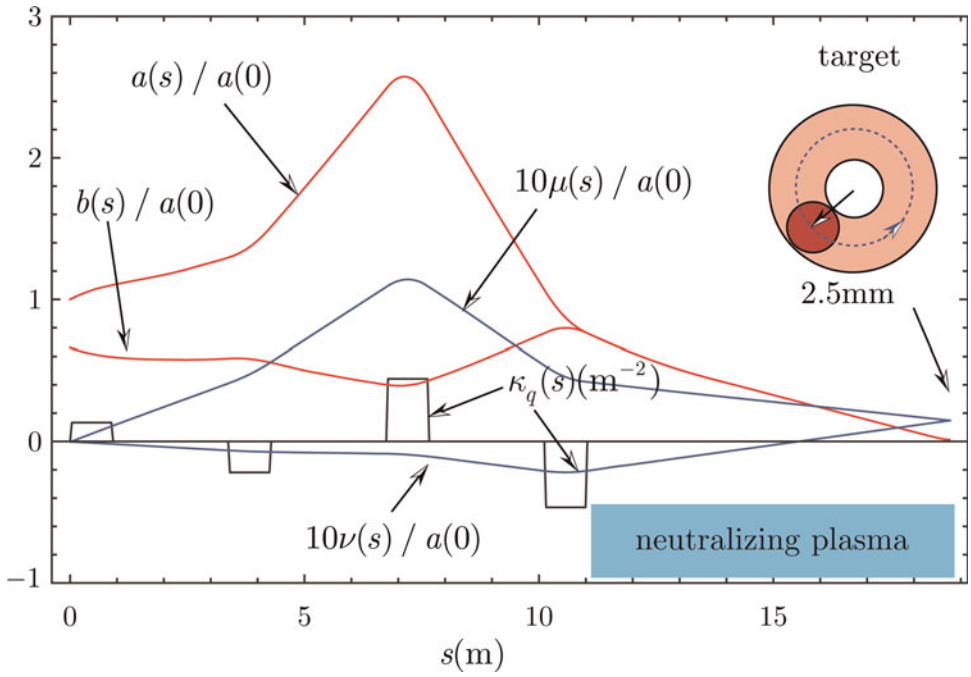


**Fig. 3.** (Color online) Final focus and wobbler system for an illustrative heavy ion fusion driver (Qin *et al.*, 2010). The radius of the centroid circle is 2.5 mm. The centroid dynamics is for the slice where $(\mu, \nu) = (1.77\ \text{mm}, 1.77\ \text{mm})$ on the target, and the normalized momentum input by the wobbler fields is $(\mu', \nu') = (6.27 \times 10^{-4}, -0.85 \times 10^{-4})$ at $s = 0$ (not shown). The vertical scale for $\kappa_q$ is $\text{m}^{-2}$. The envelope dimensions ($a$, $b$) are normalized by the initial beam envelope dimension $a(0)$. The centorid positions ($\mu$, $\nu$) are normalized by $a(0)/10$ for better illustration.

required is 0.30 MV/m, which are achievable with current technology. It is also possible to place the wobbler plates in the upstream of the beam before the longitudinal compression (Qin *et al.*, 2004), then a RF field with lower frequency can be used to achieve the desired wobbling effect on the target.

## 5. CONCLUSIONS

In summary, a fully self-consistent solution for high-intensity charged particle beams in a quadrupole lattice with wobbler fields is given by Eqs. (42), (40), and (41), and the centroid dynamics is determined from Eqs. (35) and (36). The deflection force imposed by the wobbler fields acts only on the centroid, and the self-consistent space-charge field only affects the envelope motion. This is consistent with the analysis leading to the rms envelope equations including the centroid dynamics. These conclusions and the corresponding envelope equations and centroid equations are expected to serve as theoretical tools in designing beam wobbler systems for applications to higher energy density physics and heavy ion fusion. The kinetic solution to the nonlinear Vlasov-Maxwell equations considered in Section 3 corresponds to the case where the beam has a flat-top density profile. For more general choices of beam density profiles that are not flat-top, we expect that the rms envelope equations and the centroid equations derived by taking appropriate moments of the Vlasov-Maxwell equations in Section 2 remain a good approximation, particularly if the change in beam emittance remains small (Dorf *et al.*, 2009). In the present study, we have not considered non-ideal effects that may exists in real accelerators and beam transport system. When the envelope amplitude is large, the effects associated with lens nonlinearities can couple the centroid and envelope dynamics. In addition, the error field of the wobbler should be taken into account as well. These effects need to be addressed in future study.

## ACKNOWLEDGMENTS

This research was supported by the U.S. Department of Energy.

## REFERENCES

Barnard, J. (1996). In *Proceedings of the 1995 Particle Accelerator Conferences*, p. 3241. New York: IEEE.

Bernal, S., Li, H., Kishek, R., Quinn, B., Walter, M., Reiser, M., O'Shea, P. & Allen, C. (2006). RMS envelope matching of electron beams from zero current to extreme space charge in a fixed lattice of short magnets. *Physi. Rev.: Accele. and Beams* **9**, 1–17.

Blind, B. & Gilpatrick, J.D. (2007). LANSCE-linac beam-centroid jitter in transverse phase space. In *Proceedings of 2007 Particle Accelerator Conference*, pp. 4093–4095. New York: IEEE.

Davidson, R.C. & Qin, H. (2001). *Physics of Intense Charged Particle Beams in High Energy Accelerators*. Imperial College Press and World Scientific.

https://doi.org/10.1017/S0263034611000401 Published online by Cambridge University Press

Dorf, M.A., Davidson, R.C., Startsev, E.A. & Qin, H. (2009). *Phys. Plasmas* **16**, 123107.

Friedman, A., Barnard, J., Briggs, R., Davidson, R., Dorf, M., Grote, D., Hene-Stroza, E., Lee, E., Leitner, M. & Logan, B. (2009). Towward a physics design for NDCX-II, an ion accelerator for warm dense matter and HIF target physics studies. *Nucl. Instr. Meth. Phys. Res*. **A606**, 6–10.

Hoffmann, D.H.H. (2009). Private communication.

Kapchinskij, I. & Vladimirskij, V. (1959). In *Proc. of the International Conference on High Energy Accelerators and Instrumentation*. Geneva: CERN Scientific Information Service.

Kawata, S., Sato, T., Teramoto, T., Bandoh, E., Masubichi, Y. & Takahashi, I. (1993). Radiation effect on pellet implosion and Rayleigh-Taylor instability in light-ion beam inertial confinement fusion. *Laser Part. Beams* **11**, 757.

Lee, E., Close, E. & Smith, L. (1998). In *Proceedings of the 1987 Particle Accelerator Conference*, p. 1186. New York: IEEE.

Logan, G.G. (2011). To be published.

Logan, B.G., Perkins, L.J. & Barnard, J.J. (2008). Direct drive heavy-ion-beam inertial fusion at high coupling efficiency. *Phys. plasmas* **15**, 072701.

Lund, S. & Barnard, J.J. (2009). U.S. Part. Accel. Shool lecture Notes. U.S. Part. Accel. Shool Lecture Notes.

Lund, S. & Bukh, B. (2004). Stability properties of the transverse envelope equations describing intense ion beam transport. *Phys. Revi.: Accel. Beams* **7**, 1–47.

Neuffer, D., Colton, E., Fitzgerald, D., Hardek, T., R. Macek, R.H., Plum, M., Thiessen, H. & Wang, T.S. (1992). *Nucl. Instr. Methods Phys. Res*. **A321**, 1.

Piriz, A.R., Tahir, N.A., Hoffmann, D.H.H. & Temporal, M. (2003*a*). Generation of a hollow ion beam: Calculation of the rotation frequency required to accommodate symmetry constraint. *Phys. Rev. E* **67**, 017501.

Piriz, A.R., Temporal, M., Cela, J.J.L., Tahir, N.A. & Hoffmann, D.H.H. (2003*b*). Symmetry analysis of cylindrical implosions driven by high-frequency rotating ion beams. *Plasma Phys. Cont. Fusion* **45**, 1733–1745.

Qin, H. & Davidson, R.C. (2009). In *Proceedings of the 2009 Particle Accelerator Conference*. New York: IEEE.

Qin, H., Davidson, R.C., Barnard, J.J. & Lee, E.P. (2004). Drift compression and final focus for intense heavy ion beams with nonperiodic, time-dependent lattice. *Phys. Rev.: Accele. Beams* **7**, 104201.

Qin, H., Davidson, R.C. & Logan, B.G. (2010). Centroid and envelope dynamics of highintensity charged particle beams in an external focusing lattice and oscillating wobbler. *Phy.Rev. Lett*. **104**, 254801.

Sharkov, B. (2007). Overview of Russian heavy-ion inertial fusion energy program. *Nucl. Instr. Methods Phys. Res*. **A577**, 14–30.

Sharp, W., Barnard, J. & Yu, S. (1992). *Particle Accele*. **37–38**, 205.

Skupsky, S., Kessler, T., Letzring, S. & Chuang, Y. (1993). Laser-beam pulse shaping using spectral beam deflecction. *J. Appl. Phys*. **73**, 2678.

Tahir, N.A., Hoffmann, D.H.H., Kozereva, A., Tauschwitz, A., Shutov, A., Maruhn, J.A., Neuner, P.S.U., Jacoby, J., Roth, M., Bock, R., Juranek, H. & Redmer, R. (2001) *Phys. Rev. E* **63**, 016402.

Tahir, N., Stohlker, T., Shutov, A., Lomonosov, I., Forotv, V., French, M., Nettelmann, N., Redmer, R., Piriz, A., Deutsch, C., Zhao, Y., Xu, H., Xio, G. & Zhan, P. (2010). Ultra High Compression of Water Using Intense Heavy Ion Beams: Laboratory Planetary Physics. *New. J. Phys*. **12**, 073022.

Zimmermann, R. (2004). Review of single bunch instabilities driven by an electron cloud. *Phys. Rev.: Accele. Beams* **7**, 124801.